Three-dimensional Assessment of Cardiac Motion and Deformation

Nicolas Duchateau, Bart Bijnens, Jan d'Hooge, Marta Sitges

3D Echocardiography, Second Edition

Takahiro Shiota

Three-dimensional Assessment of Cardiac Motion and Deformation

Nicolas Duchateau[1], Bart Bijnens[2,3], Jan D'hooge[3], Marta Sitges[1]

[1] Hospital Clínic, Institut d'investigacions Biomèdiques August Pi i Sunyer, Universitat de Barcelona, Spain

[2] ICREA - Universitat Pompeu Fabra, Barcelona, Spain

[3] Department Cardiovascular Sciences, Laboratory of Cardiovascular Imaging and Dynamics, KU Leuven, Belgium

Keywords: Ventricular function; Myocardial motion; Myocardial deformation; Strain (-rate) imaging; 3D Speckle tracking.

Corresponding author:

Bart Bijnens.

Information and Communications Technologies Department, Universitat Pompeu Fabra. c/ Roc Boronat 138, E08018 Barcelona, Spain.

E-mail: bart.bijnens@upf.edu

1. Introduction

Recent and on-going advances in improvement of quality and potential of echocardiography leave no doubt about its potential for assessment of myocardial mechanics during the next decade. For this purpose, echocardiography has two main advantages over other imaging modalities (apart from its non-invasiveness and its widespread use in clinical practice). Firstly, its relatively high temporal resolution (from 20 up to over >100 images per cycle for 2D sequences, around 20-40 images per cycle for 3D ones), a prerequisite for the accurate assessment of fast patterns or peak events, and an absolutely necessary condition to guarantee the physiological relevance of velocity and acceleration measurements (first and second-order temporal derivatives of displacement), or strain rate (first temporal derivate of strain). Secondly, echocardiography depicts the presence of local speckle (interference) patterns, 'attached' to the tissue, along the sequence, which allows the direct visualization of local motion and deformation and their quantification through tracking-based techniques.

The main challenges for quantifying cardiac mechanics consist in taking full advantage of this potential, in particular for 3D assessment, which nowadays starts to have a reasonable image quality and sufficient temporal resolution. Recent improvements in computing efficiency and performance of post-processing required for the tracking of local speckles are also encouraging.

In this chapter, we present an overview of the assessment and quantification of cardiac motion and deformation, and to a certain extent cardiac mechanics and function, through 3D echocardiography, with special attention on the

potential of this technique, and how to interpret and properly use it. This review complements recently published clinical [1-5] and technical [6] reviews in the same domain, and the previous version of this book [7].

2. Myocardial motion and deformation

The heart is intrinsically a multi-structural three-dimensional (3D) organ. The appearance and function of each of its substructures (e.g. the left ventricle [LV]) is highly affected by the appearance and function of its environment (e.g. the right ventricle and the left atrium, the mitral and aortic valves, and the peripheral circulation), as well as its intrinsic physiology. Therefore, even in order to reproduce the main characteristics of global cardiac function (namely the overall performance of the cardiac pump), one needs to incorporate 3D information. In current clinical practice, even simplifications of the ventricles to three-dimensional cylinders or (semi-) ellipsoids are of great help for the computation of global physiological parameters, or, in an echocardiographic perspective, volume computations. For motion and deformation assessment, these simple representations are essential to recover even the basic components of the cardiac pump in each of three physiological relevant directions, namely (for the LV): longitudinal (base-to-apex) shortening, radial (endo-to-epicardial) thickening, and circumferential shortening, rotation and shearing (*Figure 1*).

To extract and interpret these components from cardiac imaging, one needs to understand the links between global and local cardiac behavior [8], mainly:

(1) The distribution of segment shortening, rotation and shearing, is mainly determined by the local arrangement of the myofibers within

the wall, with an angle of inclination with regard to the longitudinal axis of the ventricle which varies gradually between the epicardial, mid-myocardial and endocardial layers[9].

(2) The amount of longitudinal and circumferential shortening and radial thickening is mainly determined by the wall properties, such as tissue contractility but also its composition, elasticity, incompressibility, etc. In particular, incompressibility directly relates the components along the three local directions, where longitudinal and circumferential shortening is coupled with radial thickening to preserve tissue volume.

The segmental changes, independently of global measurements, are of additional importance. An illustrative example is shown in *Figure 2*, in which global contraction of two different walls is the same, despite the presence of reduced or exaggerated local contraction on some of them (illustrating e.g. differences in the tissue viability, such as the presence of local infarct).

Given these simple considerations, a good imaging technique, and its associated post-processing, should be able to accurately recover both global and local components of wall motion and deformation. The physical quantities to represent these are displacement and strain, respectively. The first one corresponds to the difference between the position of a given point of the wall at a certain point in the cardiac cycle compared to the onset of the cycle (onset QRS complex), and is a 3D vector. The second one corresponds to a difference in elongation of a small piece of tissue around a given point of the wall, also compared to the cycle onset. *Figure 3a* illustrates this concept in 1D.

Positive/negative strain corresponds to stretching/shortening, respectively. Deformation is thus the spatial derivative of the displacement vector, which in the 3D case is a 3D tensor (3x3 matrix). Mostly, we only quantify its diagonal components, being the longitudinal, radial, and circumferential deformation (*Figure 3b*).

Area strain: the area strain has been recently proposed to assess cardiac function [10], mainly to overcome problems with assessing deformation in the radial direction, as discussed later. Area strain corresponds to the product of longitudinal and circumferential strain components, and according to the conservation of local elemental volume, should correspond to the inverse of the radial strain component. Therefore, it also can be seen as a measurement of local 'overall' deformation.

When the speed of displacement and strain are assessed, i.e. taking their temporal derivatives, velocity and strain rate are quantified (*Figure 4*).

Twisting: the concept of (left ventricular) rotation or twisting was introduced in the literature as the difference in rotation between basal and apical levels, generally quantified at end-systole [11]. Its normalization by ventricle height is known as ventricular torsion [12].

3. How to measure motion and deformation

a. Speckle tracking

Changes in local speckle patterns allow quick visual assessment of motion and deformation. It is therefore logical to use them as key feature for an

automatic tracking algorithm attempting to estimate the true motion and deformation locally.

The principle behind speckle tracking algorithms is to track local tissue patches containing some speckles, between consecutive frames. These patches are highly similar from one frame to another, as the speckle patterns are conserved across several frames. The algorithm first tries to detect the location of a given patch in the next frame, using block matching or local image similarity comparisons. The displacement of a given patch between two consecutive frames therefore corresponds to a reliable estimation of myocardial motion between these instants (*Figure 5a*). Then, motion is recovered along the whole sequence by chaining the displacements obtained for each pair of consecutive frames (*Figure 5b*). In practice, the user is asked to segment the cardiac wall at given instants (generally end-systole and/or end-diastole for both 2D and 3D). This segmentation is then further propagated along the whole sequence. Although most manufacturers provide a 'black box' with little information on the implementation, most will be based on published approaches [13-15].

Some form of this approach is now included in all major echocardiographic platforms and it (mainly the 2D version) has become widely used in the clinical community, mainly for research purposes. However, more work is still needed on further clinical validation [3].

In practice, analyzing a whole dataset may still take a non-negligible amount of time to reach reliable curves (with some practice, around 2-3min for 2D, but around 30min for 3D).

Drift artifacts may arise from the frame-to-frame accumulation of errors: the displacement recovered from one frame to the next one is only an estimation of the true displacement. The error between both is probably negligible between consecutive frames, but accumulating the estimated displacements along the cycle may result in an important amplification of these small errors. Current commercially available platforms generally perform a drift correction, which assumes that cardiac motion is cyclic, and therefore forces displacement and strain at the end of the cycle to their values at the onset of the cycle (*Figure 5c, and Figure 6*). Note that this correction does not affect myocardial velocity and strain rate, as these correspond to instantaneous information and are not affected by the accumulation of errors.

b. Other techniques

Speckle tracking is not the only existing technique for estimating myocardial motion and deformation. Other approaches include *Tissue Doppler Imaging* (TDI), measuring local myocardial velocities locally by analyzing phase shifts of the returning echoes. The great advantage of this technique is its much higher temporal resolution as compared to speckle tracking (around 200 fps). However, the technique is more angle-dependent and it is difficult to recover the full 2D or 3D velocities. The operator is thus required to align the beam parallel/orthogonal to the wall, for the recovery of longitudinal (apical view) or radial (parasternal view) velocities. Additionally, given the fixed observation

position, (manual) tracking is required to follow the cardiac wall during the cycle.

Non-rigid image registration also tracks the myocardium similar to speckle tracking, but this technique relies on the warping and matching of the full echocardiographic images[A] to recover frame-to-frame displacements, and not only the matching of blocks defined locally. This technique is widely investigated and used in the academic community, and some implementations [16,17] are available as open-source[BC], and their comparison can be found in[18,19]. Further efforts are required in terms of computational time and practicability to get wider applicability in clinical practice. Note that due to its definition (warping and matching of full images/sequences), the technique is not specific to echocardiography and may be applied to any imaging modality.

Model-based approaches integrate prior knowledge to guide the tracking process and have a better computational efficiency. A model is generally trained on a population of normal and pathologic subjects, and could integrate biomechanical properties describing myocardial motion and deformation

[A] A full echocardiographic image (moving image) is warped through a given transformation, until the warped image matches a target image (fixed image). In case the fixed and moving images are consecutive images within a cardiac cycle, the transformation for which the matching is optimal corresponds to the displacement between the two consecutive frames. Further details can be found in (Jasaityte 2013).

[B] De Craene M, Piella G. An implementation of TDFFD and LDFFD algorithms. *Insight Journal*, 2012. http://hdl.handle.net/10380/3345

[C] Dru F, Vercauteren T. An ITK implementation of the symmetric Log-domain diffeomorphic demons algorithm. *Insight Journal*, 2009. http://hdl.handle.net/10380/3060

(incompressibility, elasticity, fiber orientations, etc.) and/or statistically learnt variables that describe the main population-wise variations [20-23].

c. Advantages/disadvantages of (3D) speckle tracking

Speckle tracking is less angle-dependent compared to TDI, provides an estimation of motion and deformation in all directions, and, as part of the algorithm, automatically tracks the points of the myocardium. Note however that the technique is not completely angle-independent due to the intrinsic nature of echocardiographic images with a much lower resolution in the lateral direction compared to the beam direction (especially when using sector scanning). For accuracy and computational efficiency, some manufacturers may prefer to perform the processing early in the image reconstruction chain, on 'raw data' (either non-scan-converted or even the basic reflected radiofrequency signal), while other may process the final (DICOM) images as presented to the user. However, the conversion to Cartesian coordinates (of either the image, or the tracking output) might affect the quality of the motion and deformation estimation, in particular in the direction orthogonal to the beam.

Speckle tracking, contrary to e.g. TDI, is intensity-based and therefore highly relies on a good image quality and optimal acquisition. Poor or exaggerated contrast in the walls, the presence of acoustic shadowing or reverberations, out-of-window or drop-out artifacts are some of the main image-related factors that may lower accuracy of the tracking. Reconstruction errors (in case the images result from the fusion of several cardiac cycles) should be carefully looked at in 3D. Random noise, lower wall visibility and fuzzier

endocardial/epicardial delineations may be additional limitations for 3D tracking. The lateral/anterior wall and apical regions are particularly challenging to image in 3D (e.g. field-of-view and temporal resolution constraints in dilated hearts, or constraints in the clinical workflow hampering spending time to optimize image quality).

Finally, the spatiotemporal resolution is another major limitation for the tracking: low spatial resolution can affect the quality of the speckle patterns and their resolution, while low temporal resolution can distort measurements of fast events (in particular during isovolumic contraction and relaxation or in subjects with a high heart-rate) and the accuracy of peak-based measurements. Current 3D images still have much lower quality and spatiotemporal resolution compared to 2D. However, future improvements in 3D imaging technology promise to provide solutions for this.

The current tracking algorithms involve a large number of processing steps and assumptions that should be standardized. Differences between manufacturers exist in the definition of the myocardial segments, the intrinsic definition of strain, which part of the wall to process (e.g. endocardial border or myocardial centerline), the spatiotemporal smoothness of the estimated curves, the size of the regions of interest used to track local patterns, etc. The computation of radial strain also differs between vendors. Some prefer its estimation from area strain (the product of longitudinal and circumferential components, upon elemental volume conservation assumptions) rather than its direct estimation from 3D images with very poor resolution across the wall thickness. As a result, the output may significantly differ between

manufacturers, as reported in recent literature. The relatively good reliability of the estimation of (especially global) longitudinal parameters is often emphasized, while the recovery of radial and circumferential components is less reliable.

A joint initiative including the European Association of Cardiovascular Imaging (EACVI), the American Society Echocardiography (ASE), and academic and industrial actors has recently been initiated in order to standardize deformation assessment.

d. Recommendations for the use of 3D speckle tracking

The operator can prevent a lot of the above-mentioned limitations by carefully optimizing the acquisition process and use of the speckle tracking tools, as well as being critical with the obtained results. Interpretation should also be depending on the specific application (some typical clinical examples are presented below).

Spatiotemporal resolution and image quality: The acquisition parameters should be optimized to reach optimal image quality. Special attention needs to be paid to stitching artifacts, reverberations and out-of-sector regions. The transducer frequency can be optimized (this includes the use of harmonic imaging) to improve the quality of observed speckles and wall delineation. Temporal resolution may be increased by reducing the field-of-view to the structures of interest only, but this is not a standard recommendation, as some tools require the full ventricle to be visible (including endocardial and epicardial borders). It is also recommended to have a margin >100ms at each

side of the studied cycle when acquiring a heart beat so that especially the early events are accurately captured.

Post-processing: The speckle tracking itself may introduce artifacts, if not properly executed. Timing of events (e.g. onset of QRS/end-diastole and aortic valve closure/end-systole), if allowed by the software, should be incorporated (based on e.g. simultaneously acquired blood pool flow? Doppler) and re-adjusted when needed. Careful checking of the tracking output is required at each step when allowed by the tool: if possible, out-of-window tracked regions should be avoided, and visual inspection of the tracking (how well the user-defined segmentation is propagated along the sequence) is recommended. Frame-by-frame inspection after stopping the sequence animation may help. Re-adjustments of the segmentation are generally required to reach an acceptable result. This is relatively easy to perform in 2D, and most of the available platforms offer multi-plane 2D display for 3D sequences, where the complementarities of the different views (e.g. apical 4/2/3-chamber cuts and short-axis ones) are very useful. Smoothing, both in time and space, and drift correction, may be available. The operator should be aware of their influence on the displayed curves, in particular when peak-based measurements are required (smoothing alters shape, width and magnitude of peaks, and may fuse or hide narrow peaks). Apart from checking the quality of the tracking along the cycle as described above (for endocardial/mid-wall/epicardial delineations, if available), a second verification of the resulting traces is recommended. Keep in mind that the display of all myocardial segments on the same plot may be confusing, and the operator should check the physiological relevance of the regional patterns.

Displacement and velocity curves are generally easier for assessing the quality of the tracking.

4. Relating deformation to cardiac function: practical examples

a. Relation between myocardial deformation and ventricular size

When interpreting deformation traces, it is crucial to understand the intrinsic geometrical relation between ventricular size, stroke volume, and strain (*Figure 7* shows this for an ellipsoidal representation of the left ventricle). For a given ventricular size, increased global deformation (i.e. accumulation of local deformation) results in an increased amount of blood ejected at each beat (increased stroke volume) (*Figure 7a*). In the same way, for a given amount of global deformation, larger ventricles can eject more blood than smaller ones, resulting in an increased stroke volume (*Figure 7b*). In other words, less deformation is required from a bigger ventricle to generate the same amount of stroke volume. From a clinical point-of-view, this partially explains certain aspects of cardiac remodeling: in comparison with normal hearts, dilated hearts are actually able to (1) provide the same amount of stroke volume in case of lower deformation (illustrated in *Figure 7a*, a clinical example related to this would be reduced contractility resulting from ischemia) or (2) eject more blood if required with the same amount of deformation (illustrated in *Figure 7b*, a clinical example related to this would be mitral regurgitation).

b. Normal deformation patterns

Figures 8 and *9* (and *videos 1* and *2*) show the output of the 3D deformation analysis for a healthy person: multi-view representation of 2D planes composing the 3D image (*video 1*), illustration of the endocardial and epicardial tracking (*video 2*), and the longitudinal, circumferential and radial components of deformation (traces: *figure 8* and Bull's eyes *figure 9*). The influence of drift compensation for this subject was illustrated in *Figure 6*.

The studied subject had good image quality, and the full left ventricle could be included in the field-of-view despite lower visibility of the apical lateral segments. Normal deformation patterns (contraction/relaxation phases) are easily visible, and there is the expected spatial uniformity of strain. Note however that the different phases of diastole are harder to assess as compared with the 2D measurements of *Figure 4*, a possible reason for this being the lower temporal resolution and potentially different temporal smoothing.

c. Coronary artery disease (CAD) and myocardial infarction

Patients with CAD may have locally altered deformation of the myocardium resulting from a perfusion deficit, with strong or almost total attenuation of the strain components in the (chronic) infarct zone, if present. Additionally, the presence of post-systolic deformation is an important feature to quantify when assessing CAD patients [24]. While delayed enhancement cardiac magnetic resonance can provide a clear delineation of the scar, 3D myocardial deformation imaging may be used as a surrogate for this, with the additional advantage that global strain measurements can be used as an estimation of

global cardiac function. *Figures 10* and *11* (and *video 3*) show similar information as before to assess local alterations of the 3D strain patterns in one patient with a basal inferior infarct. Low strain is observed at the scar location, together with alterations in the neighboring segments.

d. Hypertrophy

Myocardial deformation may be strongly reduced in patients with cardiac hypertrophic cardiomyopathy (HOCM). Additionally, different hypertrophic substrates show clearly distinct and specific changes in regional shape of the deformation trace [2]. Similarly to the previous case, 3D quantification of the local alterations of the strain patterns may be useful for the identification of the hypertrophic etiology and the estimation of local wall performance and global cardiac function. *Figures 12* and *13* (and *video 4)* show the deformation for a HOCM patient. Segments with major hypertrophy show lower deformation, in comparison with higher strain magnitude observed in the neighboring segments.

e. Mechanical dyssynchrony: left bundle branch block example

The specific and complex motion and deformation patterns in the context of left bundle branch block (LBBB), and the importance of their understanding for cardiac resynchronization therapy (CRT), has been described in 2D [25-30]. Despite the possible difficulty to image these patients in 3D (dilated hearts and presence of fast motion patterns), 3D motion and deformation quantification is feasible in these patients. *Figure 14* and *15* (and *video 5*) show the specific deformation in a CRT candidate with LBBB and intra-

ventricular mechanical dyssynchrony, as visible by the presence of a fast inward-outward motion of the septum during the isovolumic contraction, (septal flash or rebound stretch). 3D aids in assessing the spatiotemporal location of deformation abnormalities which is more difficult in 2D: early-systolic fast inward motion, immediately followed by outward motion and abnormal deformation (longitudinal stretching and radial shortening) of the septum, while lateral contraction comes later and is accompanied by end-systolic septal stretch.

5. Limitations and future developments

This chapter presented an overview of the assessment of cardiac mechanics through motion and deformation quantification, with special emphasis on 3D wall motion quantification through speckle tracking. As cardiac mechanics is intrinsically 3D, the advantages of 3D echocardiography over 2D are straightforward. While current tools might not be fully ready for being used in clinical routine due to technological limitations (frame rate, image quality, tracking accuracy), cautious use and appropriate training (to optimize image quality and reduce the duration of the echocardiographic examination) and intensive use of the software tools (frame-to-frame checking and manual corrections) may help achieving a comprehensive assessment of the spatiotemporal changes in local deformation patterns, in relation with the pathophysiology of the observed subject.

Acknowledgements

Funding

This work was partially supported by the Spanish Industrial and Technological Development Center (cvREMOD CEN-20091044) and by the Subprograma de Proyectos de Investigación en Salud, Instituto de Salud Carlos III, Spain (FIS - PI11/01709).

Conflict of interest

None.

References

(1) Bijnens BH, Cikes M, Claus P, et al. Velocity and deformation imaging for the assessment of myocardial dysfunction. *Eur J Echocardiogr*, 2009;10:216-26.

(2) Cikes M, Sutherland GR, Anderson LJ, et al. The role of echocardiographic deformation imaging in hypertrophic myopathies. *Nat Rev Cardiol*, 2010;7:384-96.

(3) Mor-Avi V, Lang RM, Badano LP, et al. Current and evolving echocardiographic techniques for the quantitative evaluation of cardiac mechanics. *J Am Soc Echocardiogr*, 2011;24:277-313.

(4) Bijnens B, Cikes M, Butakoff C, et al. Myocardial motion and deformation: what does it tell us and how does it relate to function? *Fetal Diagn Ther*, 2012;32:5-16.

(5) Cheung YF. The role of 3D wall motion tracking in heart failure. *Nat Rev Cardiol*, 2012;9:644-57.

(6) Jasaityte R, Heyde B, D'hooge J. Current State of Three-Dimensional Myocardial Strain Estimation Using Echocardiography. *J Am Soc Echocardiogr*, 20--; in press.

(7) Stoylen A. Strain echocardiography. In: Shiota T, ed. *3D echocardiography*. Informa Healthcare, 2007:141-51.

(8) Buckberg G, Hoffman JI, Mahajan A, et al. Cardiac mechanics revisited: the relationship of cardiac architecture to ventricular function. *Circulation*. 2008;118:2571-87.

(9) Vendelin M, Bovendeerd PH, Engelbrecht J, et al. Optimizing ventricular fibers: uniform strain or stress, but not ATP consumption, leads to high efficiency. *Am J Physiol Heart Circ Physiol*, 2002;283:H1072-81.

(10) Seo Y, Ishizu T, Enomoto Y, et al. Endocardial surface area tracking for assessment of regional LV wall deformation with 3D speckle tracking imaging. *JACC Cardiovasc Imaging*, 2011;4:358-65.

(11) Ashraf M, Zhou Z, Nguyen T, et al. Apex to base left ventricular twist mechanics computed from high frame rate two-dimensional and three-dimensional echocardiography: a comparison study. *J Am Soc Echocardiogr*, 2012;25:121-8.

(12) Henson RE, Song SK, Pastorek JS, et al. Left ventricular torsion is equal in mice and humans. *Am J Physiol Heart Circ Physiol*, 2000;278:H1117-23.

(13) Adam D, Landesberg A, Konyukhov E, et al. On changing coordinate systems for longitudinal tensor-based morphometry. *Proc. IEEE Computers in Cardiology*, 2004;337-40.

(14) Behar V, Adam D, Lysyansky P, et al. The combined effect of non- linear filtration and window size on the accuracy of tissue displacement estimation using detected echo signals. *Ultrasound*, 2004;41:743-53.

(15) Leitman M, Lysyansky P, Sidenko S, et al. Two-dimensional strain-a novel software for real-time quantitative echocardiographic assessment of myocardial function. *J Am Soc Echocardiogr*, 2004;17:1021-9.

(16) De Craene M, Piella G, Camara O, et al. Spatiotemporal diffeomorphic free-form deformation: application to motion and strain estimation from 3D echocardiography. *Med Image Anal*, 2012;16:427-50.

(17) Vercauteren T, Pennec X, Perchant A, et al. Diffeomorphic demons: efficient non-parametric image registration. *Neuroimage*, 2009;45:S61-72.

(18) Klein A, Andersson J, Ardekani BA, et al. Evaluation of 14 nonlinear deformation algorithms applied to human brain MRI registration. *Neuroimage*, 2009;46:786-802.

(19) Tobon-Gomez C, De Craene M, McLeod K, et al. Evaluation of current algorithms for myocardial tracking and deformation: Cardiac motion analysis challenge. *Medical Image Analysis*, 2013; in press.

(20) Lorenz C, von Berg J. A comprehensive shape model of the heart. *Med Image Anal*, 2006;10:657-70.

(21) Zheng Y, Barbu A, Georgescu B, et al. Four-chamber heart modeling and

automatic segmentation for 3-D cardiac CT volumes using marginal space learning and steerable features. *IEEE Trans Med Imaging*, 2008;27:1668-81.

(22) Sheehan FH, Kilner PJ, Sahn DJ, et al. Accuracy of knowledge-based reconstruction for measurement of right ventricular volume and function in patients with tetralogy of Fallot. *Am J Cardiol*, 2010;105:993-9.

(23) Hoogendoorn C, Duchateau N, Sanchez-Quintana D, et al. A High-Resolution Atlas and Statistical Model of the Human Heart from Multislice CT. *IEEE Trans Med Imaging*, 20--; in press.

(24) Bijnens BH, Claus P, Weidemann F, et al. Investigating cardiac function using motion and deformation analysis in the setting of coronary artery disease. *Circulation*, 2007;116:2453-64.

(25) Bijnens B, Claus P, Parsai C, et al. Assessing cardiac function in dilated and failing hearts. In: Sutherland GR, Hatle L, Claus P, D'hooge J, Bijnens B, eds. *Doppler myocardial imaging, a textbook*. Belgium: BSWK- Hasselt, 2006:251–77.

(26) Parsai C, Bijnens B, Sutherland GR, et al. Toward understanding response to cardiac resynchronization therapy: Left ventricular dyssynchrony is only one of multiple mechanisms. *Eur Heart J* 2009;30:940-9.

(27) Duchateau N, Doltra A, Silva E, et al. Atlas-based Quantification of Myocardial Motion Abnormalities: added-value for Understanding the effect of Cardiac Resynchronization Therapy. *Ultrasound Med Biol*, 2012;38:2186-97.

(28) Leenders GE, Lumens J, Cramer MJ, et al. Septal deformation patterns delineate mechanical dyssynchrony and regional differences in contractility: Analysis of patient data using a computer model. *Circ Heart Fail* 2012;5:87–96.

(29) Lumens J, Leenders GE, Cramer MJ, et al. Mechanistic evaluation of echocardiographic dyssynchrony indices: Patient data combined with multi-scale computer simulations. *Circ Cardiovasc Imaging* 2012;5:491-9.

(30) Tobon-Gomez C, Duchateau N, Sebastian R, et al. Understanding the mechanisms amenable to CRT response: from pre-operative multimodal image

data to patient-specific computational models. *Med Biol Eng Comput*, 20--; in press.

Tables

No table.

Figure legends

Figure 1: The three components of myocardial motion and deformation: longitudinal, radial, and circumferential.

Figure 2: Importance of the quantification of both global and local deformation: two walls shortening equally overall (75% of their initial length), but with very different local behavior due to different tissue viability.

Figure 3: Illustration of the strain concept in 1D (left) and 3D (right). In 3D, diagonal components relate to forces orthogonal to the elemental surface, while non-diagonal components (shearing) relate to forces parallel to the elemental surface.

Figure 4: From left to right: longitudinal displacement, velocity, strain and strain rate for one healthy volunteer, at basal- (top), mid- (middle) and apical-septal (bottom) levels (from 2D speckle tracking). Vertical bars indicate the physiological events of the cardiac cycle: beginning and ending of the cycle (Q1 and Q2), mitral and aortic valve opening and closure (MVO/MVC and AVO/AVC).

Figure 5: Conservation of local speckle patterns over consecutive frames, allowing the assessment of local motion and deformation (left). Illustration of the link between displacement and instantaneous velocities (middle). The accumulation of small errors along the sequence may require compensating for drifting (right).

Figure 6: Illustration of the effect of drift correction for one healthy volunteer (3D speckle tracking): the lack of drift compensation may bias the quantification of the recovered curves (in this case, spatial uniformity of deformation and magnitude).

Figure 7: Relation between ventricular size (end-diastolic volume), stroke volume, and deformation (longitudinal strain), estimated from an ellipsoid model of the left ventricle. (Modified from Bijnens 2012).

Figure 8: Healthy subject. Longitudinal/circumferential/radial/area strain traces, after drift correction.

Figure 9: Healthy subject. Corresponding bull's eye representation.

Figure 10: CAD patient. Longitudinal/circumferential/radial/area strain traces, after drift correction. Infarcted segment: basal-inferoseptal.

Figure 11: CAD patient. Corresponding bull's eye representation.

Figure 12: HOCM patient. Longitudinal/radial strain traces, after drift correction. Hypertrophic segments: mid-anteroseptal and mid-inferolateral. Neighboring segments: apical-anteroseptal and basal-inferoseptal.

Figure 13: HOCM patient. Corresponding bull's eye representation.

Figure 14: LBBB patient. Longitudinal/radial strain traces, after drift correction.

Figure 15: LBBB patient. Corresponding bull's eye representation.

Video 1: Healthy subject. Multi-view representation of 2D planes composing the 3D image: apical 4/2/3-chamber and apical/mid/basal short-axis views.

Video 2: Healthy subject. Endocardial and epicardial tracking achieved through commercial 3D speckle tracking software. Manual re-adjustments were necessary at each stage of the tracking (end-systole/diastole endocardial/epicardial segmentations and propagation of the delineation along the whole sequence), and are identified in some frames by green circles.

Video 3: CAD patient. Multi-view representation of 2D planes composing the 3D image: apical 4/2/3-chamber and apical/mid/basal short-axis views.

Video 4: HOCM patient. Multi-view representation of 2D planes composing the 3D image: apical 4/2/3-chamber and apical/mid/basal short-axis views.

Video 5: LBBB patient. Multi-view representation of 2D planes composing the 3D image: apical 4/2/3-chamber and apical/mid/basal short-axis views.

Artwork for figures

Figure 1

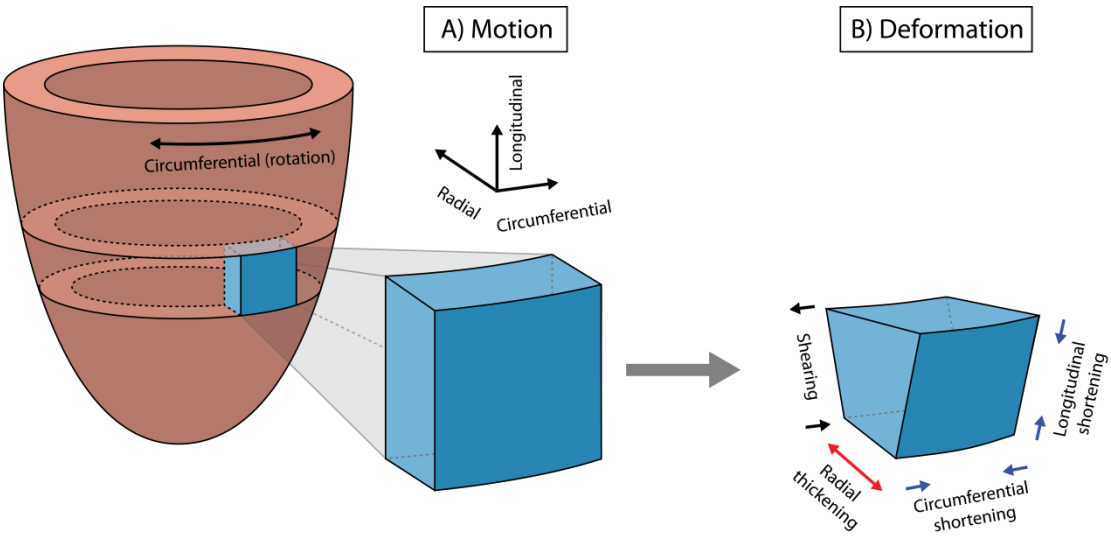

Figure 2

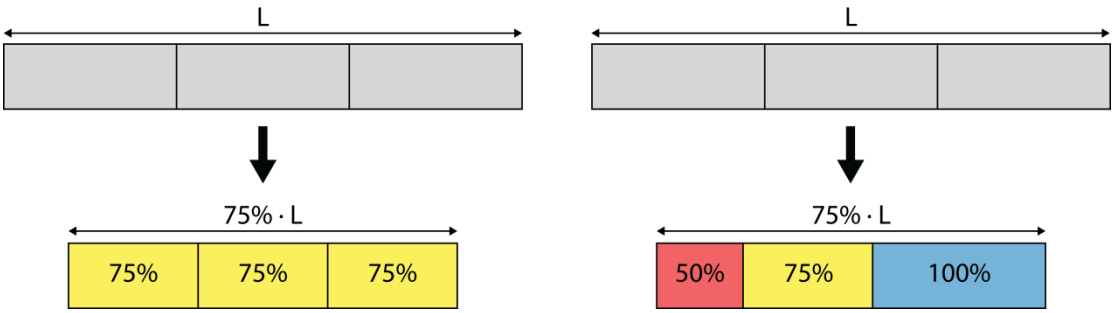

Figure 3

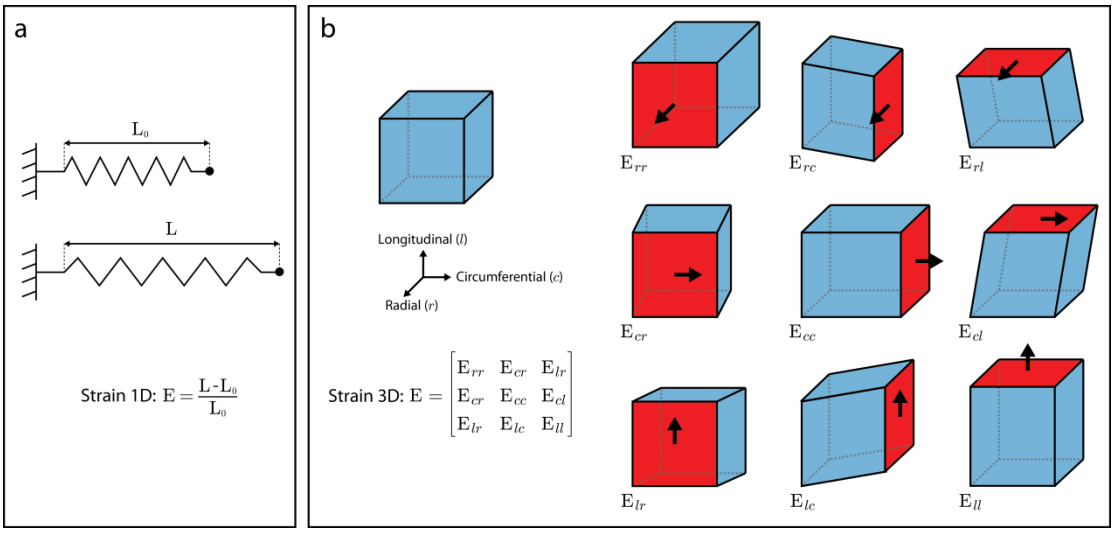

Figure 4

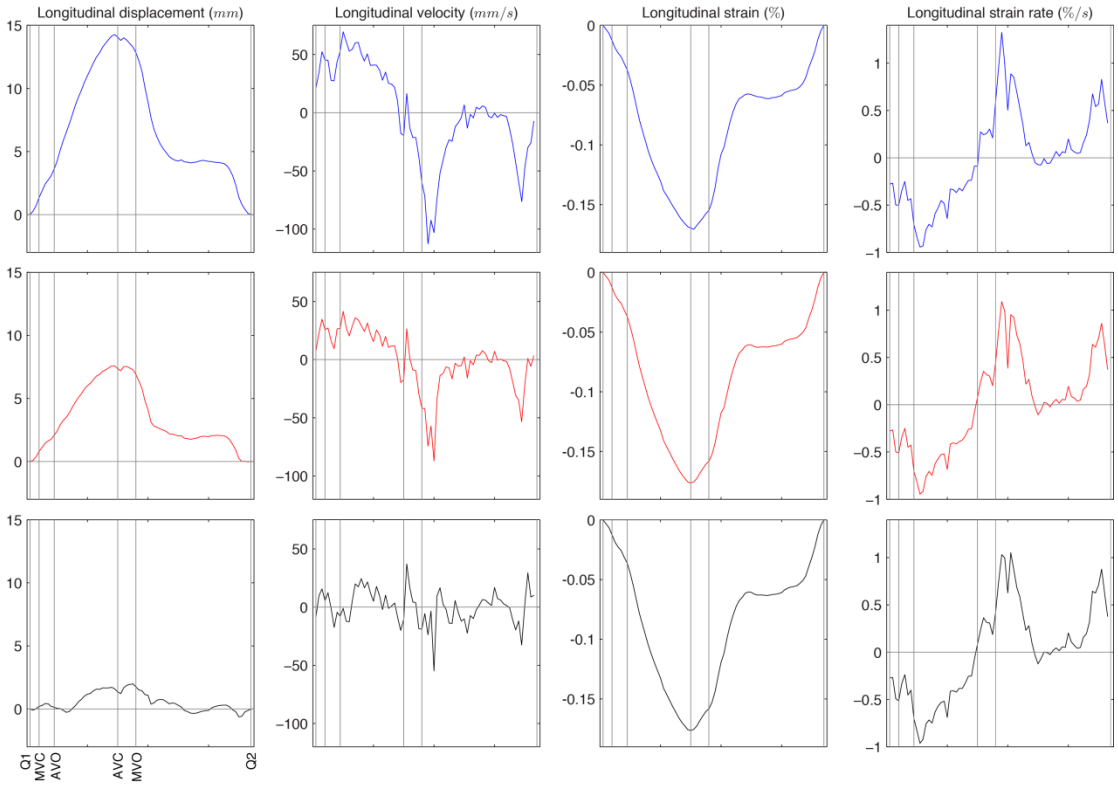

Figure 5

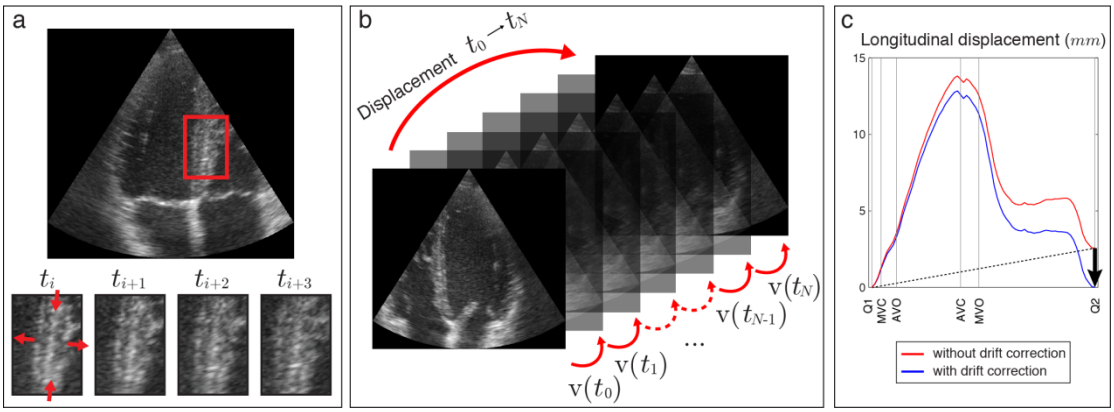

Figure 6

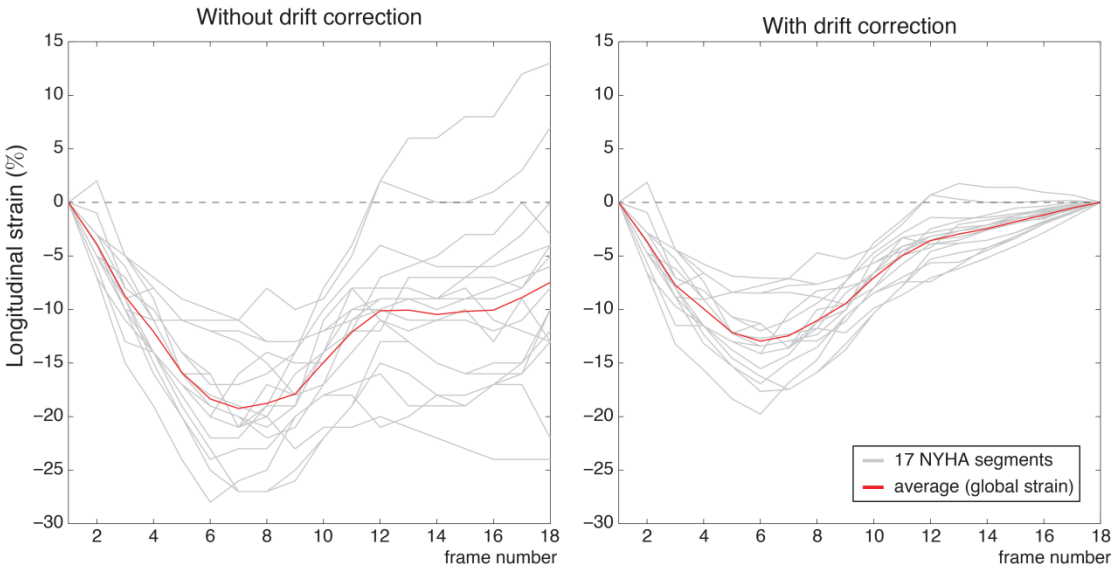

Figure 7

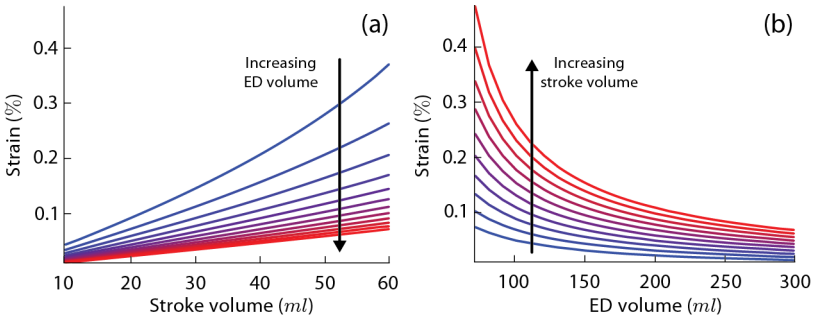

Figure 8

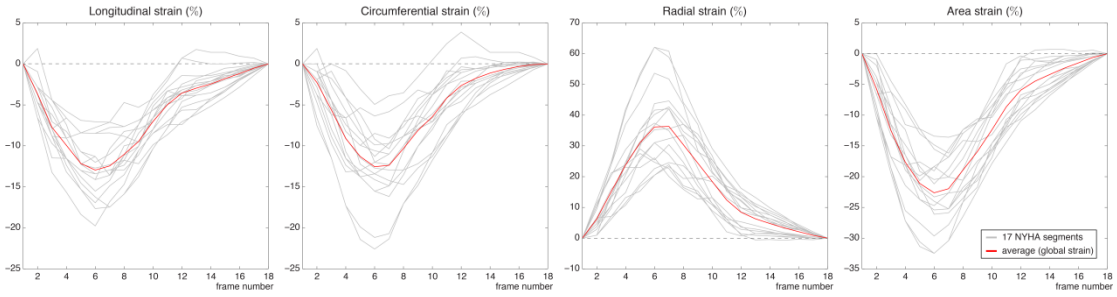

Figure 9

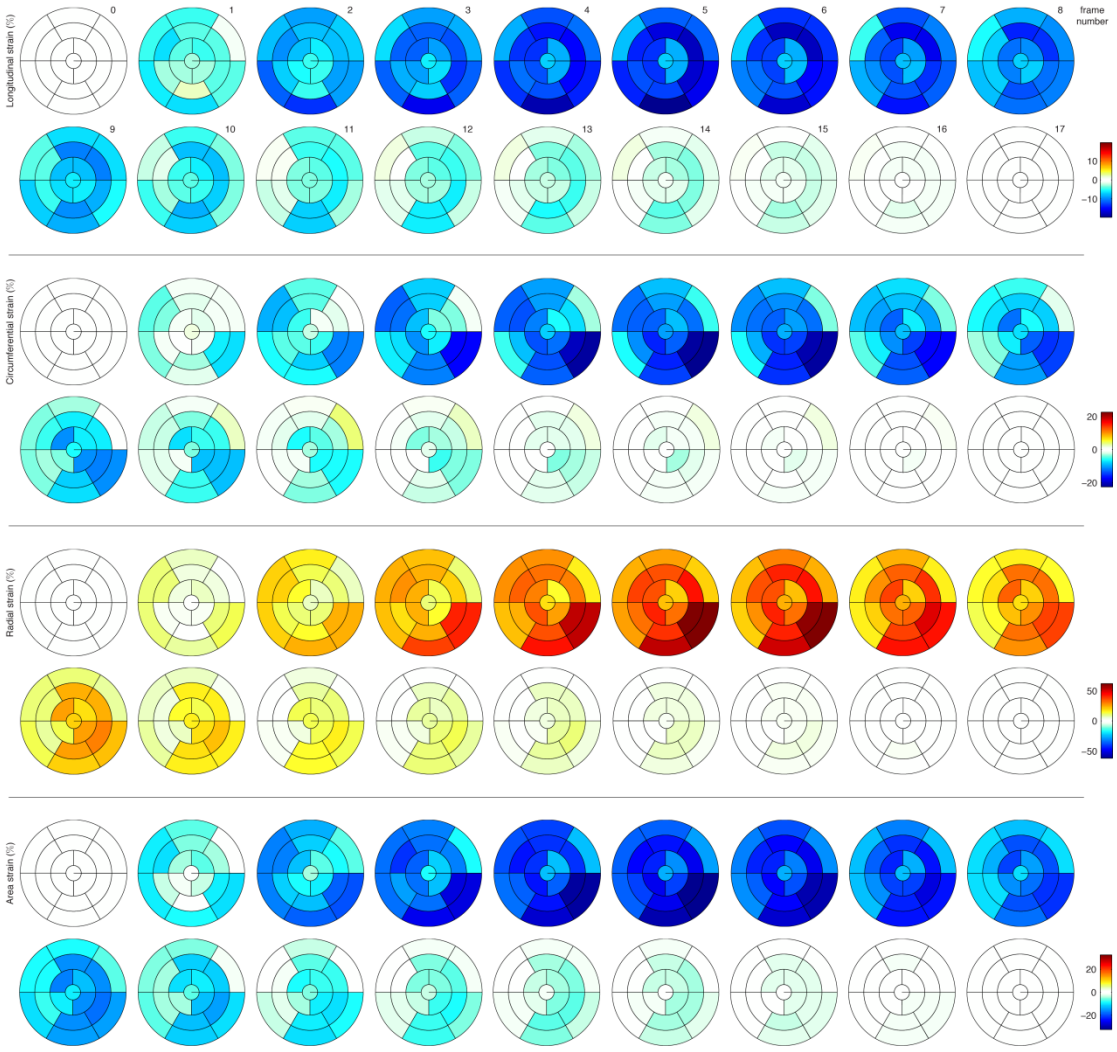

Figure 10

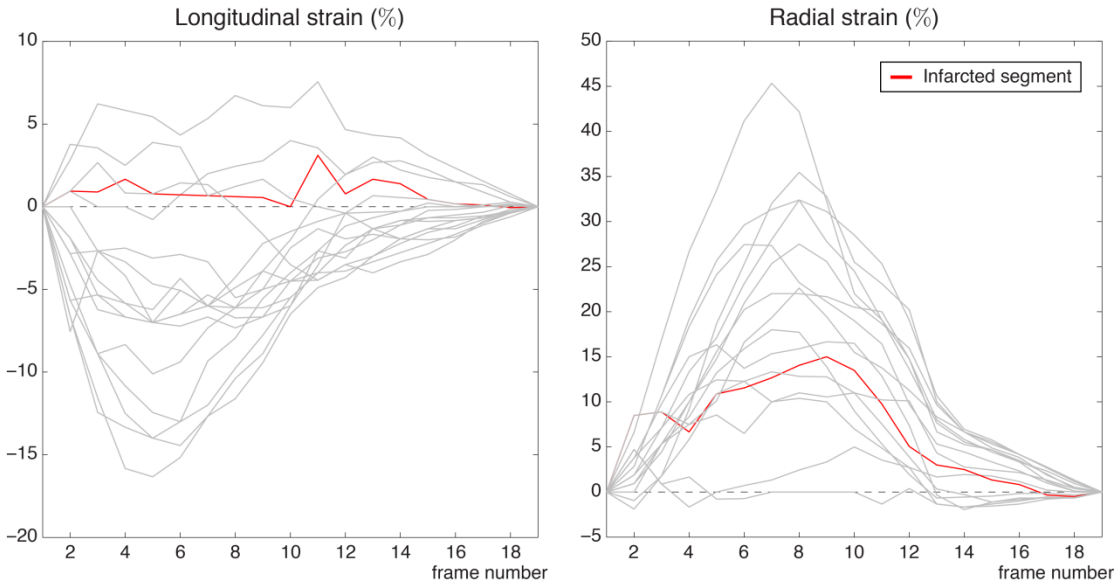

Figure 11

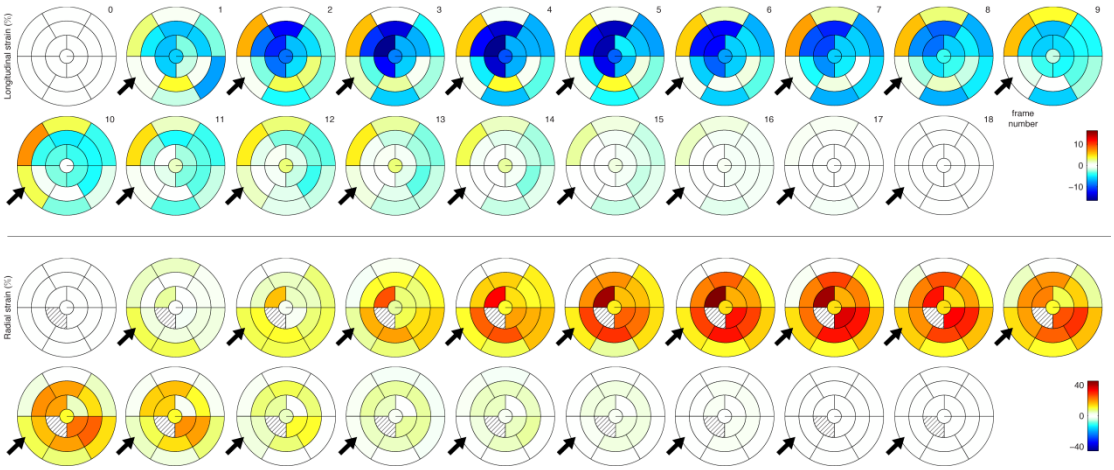

Figure 12

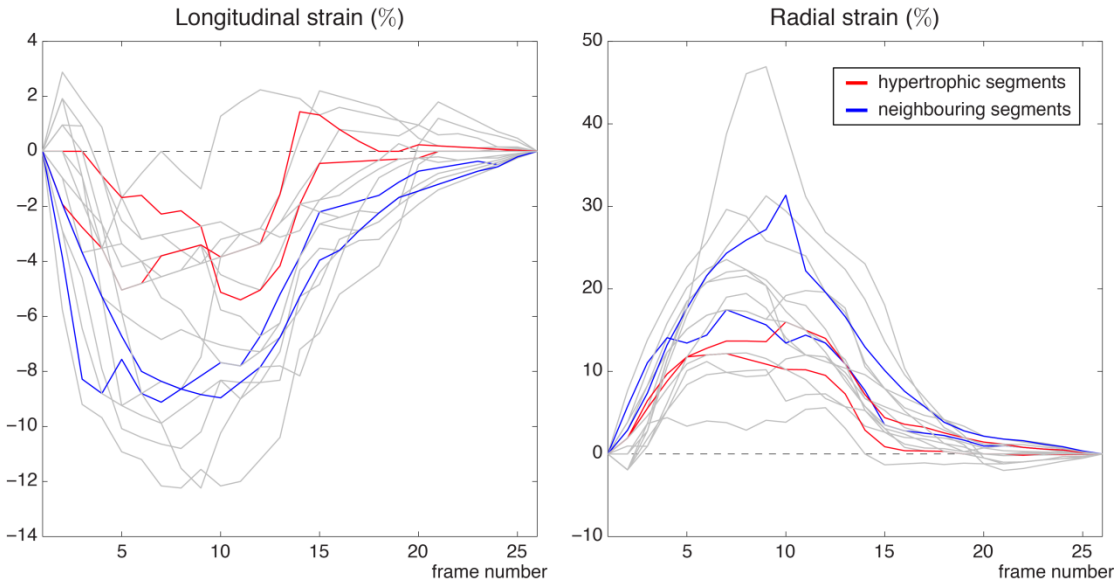

Figure 13

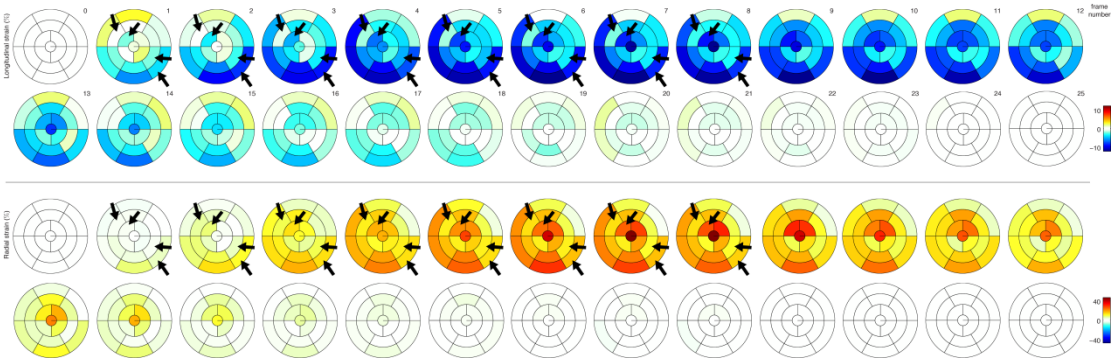

Figure 14

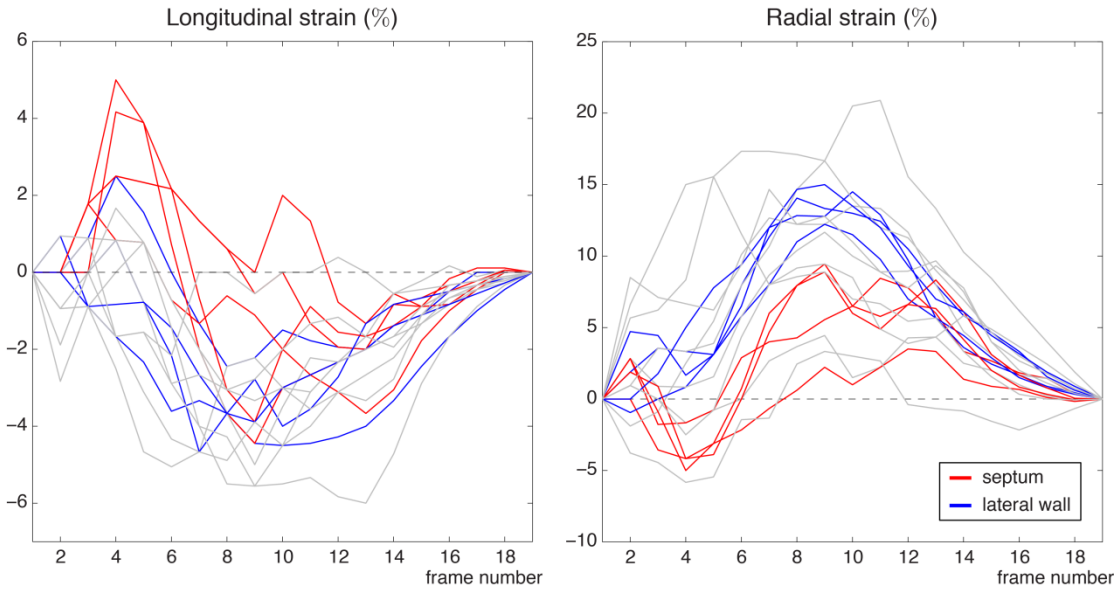

Figure 15

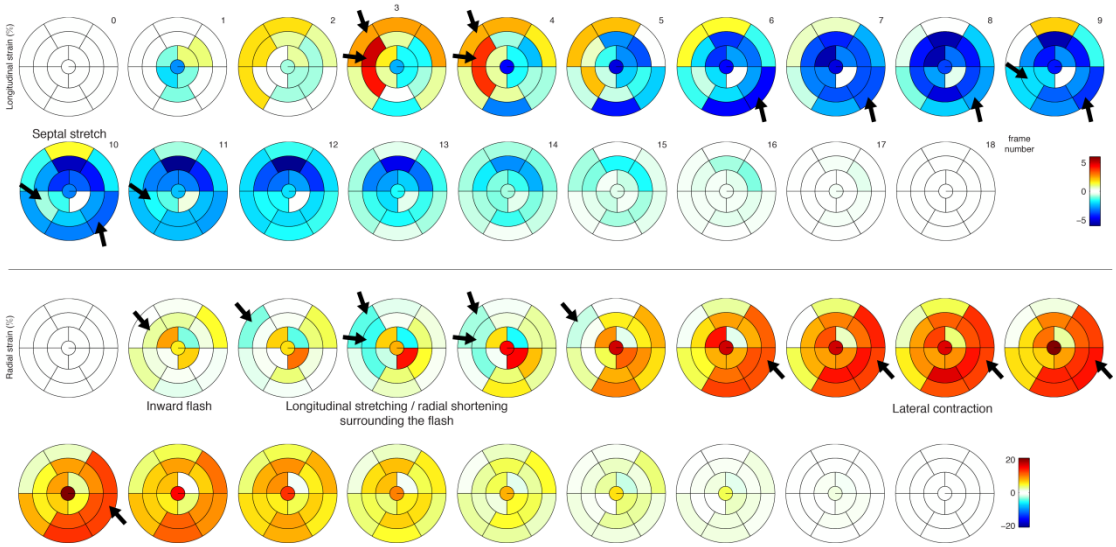

Video material

Video 1

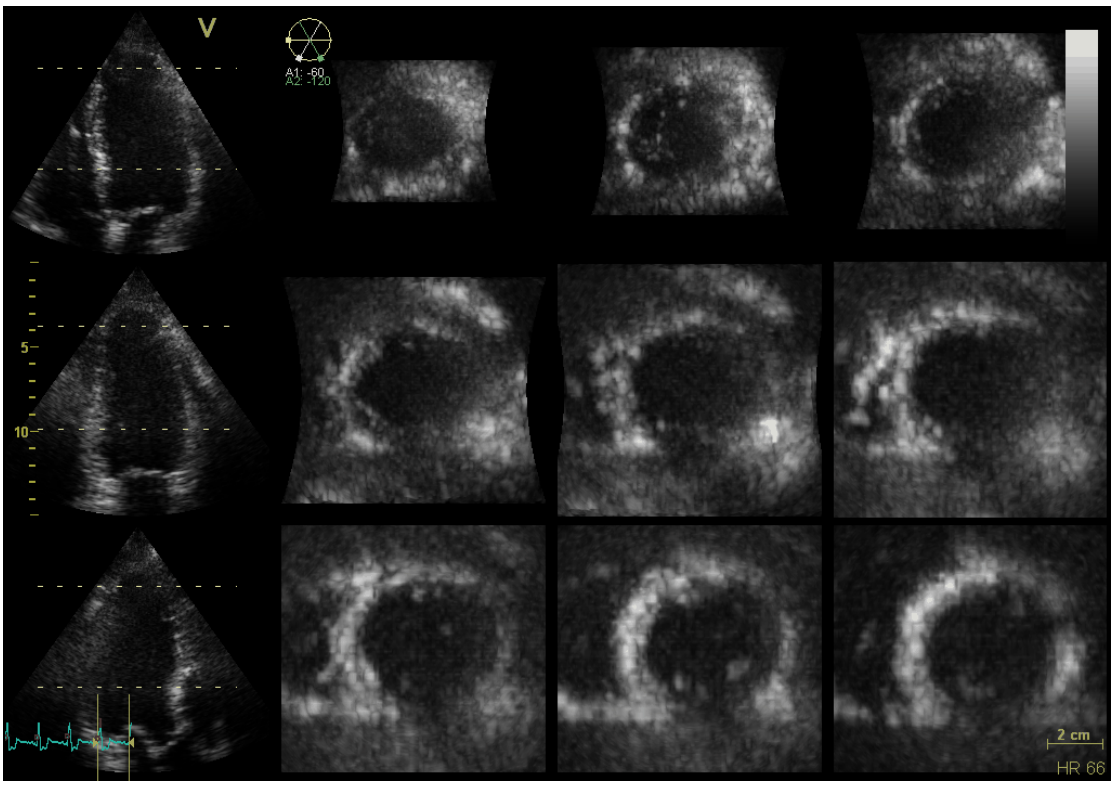

Video 2

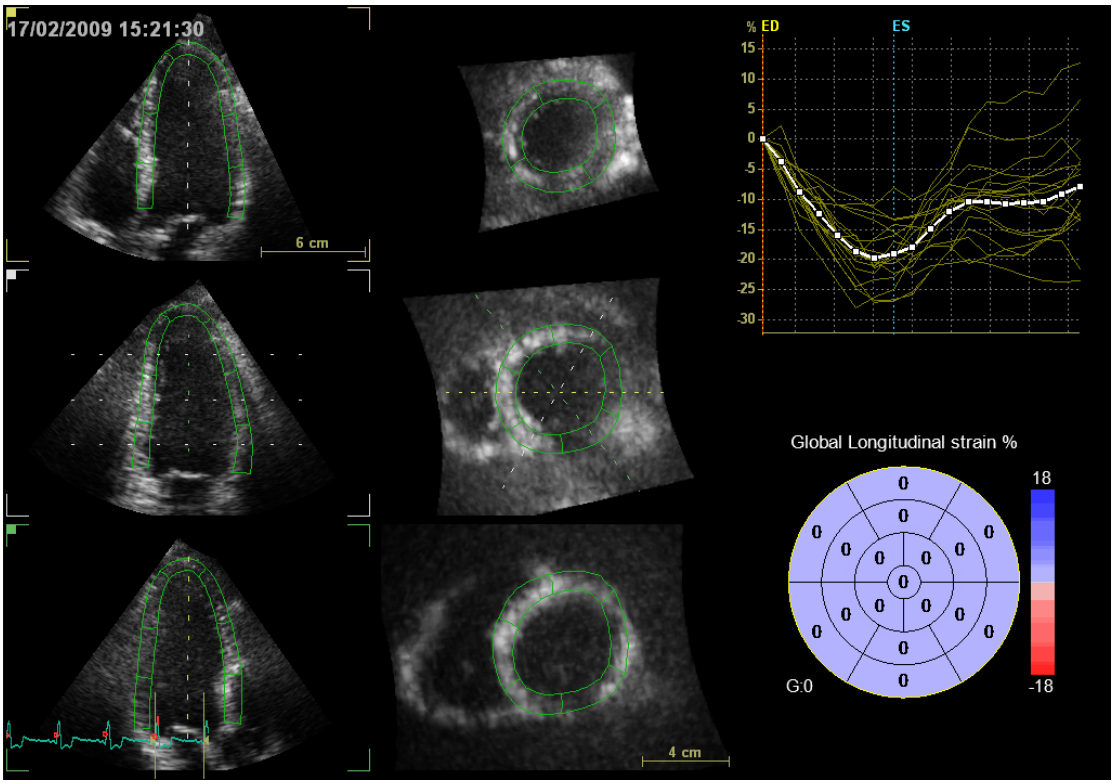

Video 3

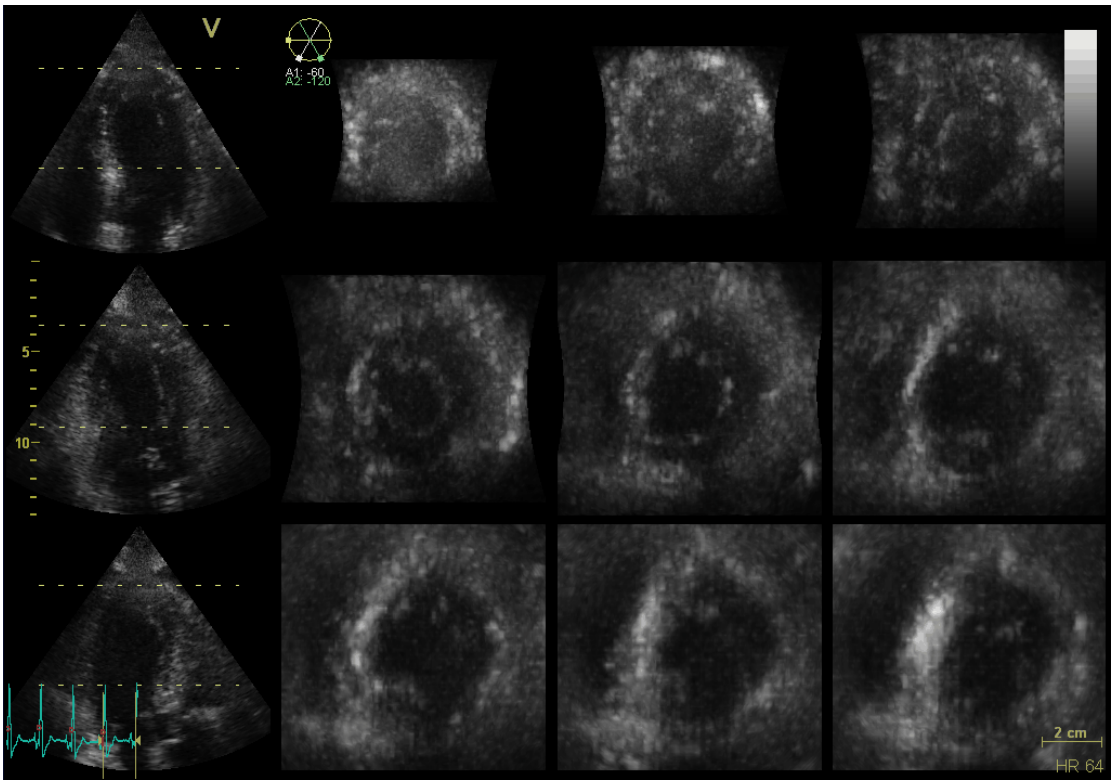

Video 4

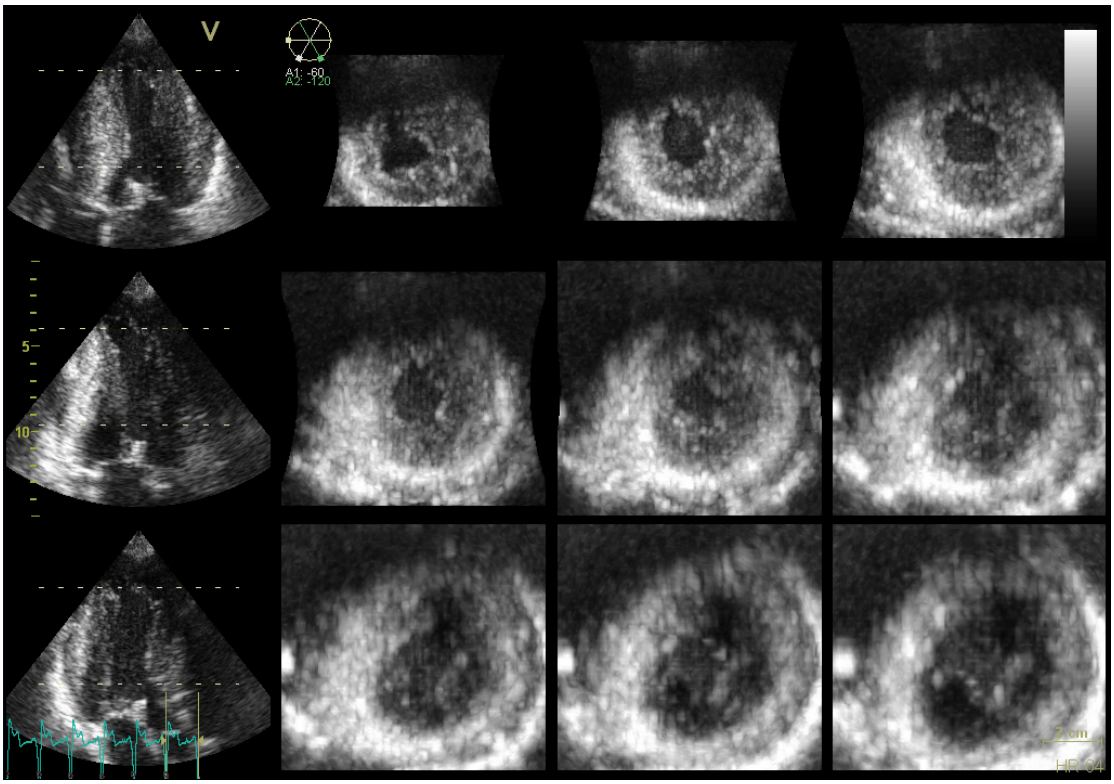

Video 5